IMA Journal of Applied Mathematics (2017) 1–20
doi: 10.1093/imamat/hxh000

Effect of random forcing on fluid lubricated bearing

N. Y. Bailey*
Department of Mechanical Engineering, University of Bath, Bath, BA2 7AY, UK
S. Hibberd and M. Tretyakov
School of Mathematical Sciences, University of Nottingham, Nottingham, NG7 2RD, UK
and
H. Power
Faculty of Engineering, University of Nottingham, Nottingham, NG7 2RD, UK
* *Corresponding author: N.Y.Bailey@bath.ac.uk*

[Received on]

A model for a fluid lubricated bearing is derived for operation under conditions where external forces are subject to random fluctuations that may act to destabilise the bearing. The fluid flow through the bearing is described by a Reynolds equation for incompressible flow and is coupled to the axial displacement of the bearing faces as modelled by spring-mass-damper systems. Representative dynamics of a highly rotating bearing subject to external potentially destabilising random forcing is developed. An external force characterised by a noise term is imposed on the rotor, where both white noise and coloured noise are considered. For industrial applications it is important to evaluate potential bearing failure that can arise when the face clearance becomes sufficiently small. Therefore, a quantity of interest is the average time for the face clearance to reach a prescribed tolerance. A computational technique to evaluate the bearing characteristics is implemented based on a simple random walk for a Dirichlet problem for a linear parabolic partial differential equation combined with a Monte Carlo technique. Results of numerical experiments are presented, to give indicative predictions of possible face contact, which has the potential to result in bearing failure.

Keywords: Reynolds equation, fluid lubricated bearing, random forcing, random walk, Monte Carlo technique

1 Introduction

Fluid lubricated bearings comprise of two structural components, a rotor and a stator which are separated by a thin fluid film. Generally the intrinsic bearing film dynamics are employed to maintain a suitable gap between the rotating and stationary elements when external axial loads are applied. In a stable configuration the squeeze-film dynamics provide an increase in the fluid film pressure, corresponding to an increase in the fluid force on the bearing faces. Typically such fluid lubricated bearings operate with smaller tolerances than traditional bearings and require a sufficient face clearance to be maintained in order to avoid possible face contact and potential bearing failure.

The concept of a squeeze film bearing introduced by Salbu (1964), who examined bearings under operation in highly vibrational environments which had significant axial disturbances. Malanoski & Waldron (1973) investigated the feasibility of using fluid lubricated technology

for aero-engine use, where air-flow between the annuli rotor and stator was driven by a pressure gradient. Recently, investigations of fluid lubricated bearings have continued in many areas of specialist turbomachinery applications, see San Andrés & Chirathadam (2011); San Andrés & Kim (2008) including gas turbine engines as described in Crudgington *et al.* (2012).

Early work by Green & Etison (1983) identified the importance of the dynamic behaviour of the fluid film. For models to capture the complete dynamics of the bearing, the fluid flow must be suitably coupled to the structural components. A coupled three dimensional model of a fluid lubricated device was formulated by Etison (1982), where the hydrodynamic and hydrostatic components of the air film pressure were determined; the hydrostatic component incorporated the squeeze film pressure. It was concluded that the squeeze film behaviour of the fluid film can potentially maintain a clearance between the rotor and stator. Salbu (1964) examined similar geometry in a highly vibrating operational environment, specifically when experiencing significant axial disturbances where the clearance between the rotor-stator is oscillatory. Results showed that increasing the amplitude of the axial oscillations gave an increased squeeze film load carrying capacity, due to the air film pressure and force increasing.

Analysis of a simple fluid film bearing is given by Garratt *et al.* (2012) in which the pressurised fluid flow is coupled to the dynamic bearing structure. The bearing dynamics were investigated for a non-ideal operating environment where vibrations or disturbances, which could potentially destabilise the bearing operation, were modelled through prescribed periodic axial oscillations of the rotor. The amplitude of oscillations was taken to be less than the equilibrium face clearance and the stator moves axially in response to the resulting fluid film dynamics; no face contact in this case was predicted.

A similar geometry was considered by Bailey *et al.* (2013) for incompressible flow and included more extensive analytical investigations. Notably, this work also studied prescribed axial oscillations of the rotor including amplitudes larger than the equilibrium film thickness. For a bearing with parallel faces, it was found that the face clearance always remains positive, however the clearance gap can become very small. In an industrial application a minimum gap is required to avoid bearing failure as a result of surface roughness, contamination or bearing distortion.

For a more comprehensive model of a high-speed fluid lubricated bearing, additional effects could be included in the fluid film model, however, this greatly increases the model complexity. These effects include inertial effects (Bailey *et al.* (2018)), surface roughness (Varney (2017)), thermal effects (Blasiak (2015)), non-axisymmetric/three dimensional geometry (Green (2002)) and possible surface features, for example spiral grooves (Chen *et al.* (2018)) or modified surface topographies (Blasiak & Zahorulko (2016)). These effects are neglected in the current work as they are secondary effects; a simpler fluid film model allows results to be obtained which reflect the main characteristics of the technology without being overburden with additional complexity of these secondary effects.

Huang (2007) examined the dynamics of a coupled gas journal bearing corresponding to a small disturbance and velocity slip boundary conditions. The bearing stability was also shown to decrease, due to reduced dynamic coefficients, resulting in possible contact between the shaft and housing. Small axial rotor disturbances to a non-axisymmetric coupled thrust bearing was examined by Park *et al.* (2008).

Bearings placed within an operating environment may be subject to a broader range of more extensive external disturbances. Correspondingly, there is increased interest in the use of uncertainty quantification approaches to give a greater predictability of the dynamic behaviour

in industrial bearing designs to ensure safe operating conditions. A simplified case of modelling the effect of periodic excitations on a dynamical system has been examined by Hou *et al.* (1996), where the amplitude was described as a random variable with prescribed mean and standard deviation, enabling exact solutions to be found. A similar approach was implemented by Bailey *et al.* (2015) for the case of a coned bearing with slip boundary conditions to examine the probability of face contact. The dynamic rotor axial displacement was prescribed by axial periodic oscillations with amplitude described by a probability distribution function with given mean and standard deviation. This work showed that the rotor displacement could be larger than the equilibrium face clearance.

Experimental studies of the dynamic behaviour of a fluid lubricated bearing, termed non-contacting face seal in the literature, has been limited to date. Etsion & Burton (1979) and Etsion & Constantinescu (1984) were among the first to develop an experimental rig with a flexibly mounted stator and examined the motion of the sealing rings. The phenomena of self-excited oscillations and large amplitude wobble were identified. Further, Metcalfe (1982) identified a half-frequency whirl in the case of the flexibly mounted stator following the rotor angular misalignment. Similar experiments have been conducted by Lee & Green (1994, 1995), but in this case with a flexibly mounted rotor. Results showed that the nonlinearities in the system can cause higher harmonic oscillations and relative angular misalignment, but optimising the seal parameters can lead to safe non-contacting seal operation. The same experimental rig was used by Zou & Green (1999); Zou & et al. (2000); Zou & et al. (2000) to investigate the dynamic responses of axial and angular modes, attempting to eliminate contact between the faces by reducing the relative maximum relative misalignment. Additionally, Green (2001) monitored the dynamic behaviour of the seal, and by changing the fluid film stiffness and damping coefficients, controlled the closing force in real time. More recently, Chen *et al.* (2018) examined the transient-state film thickness and leakage rate of a dry gas seal at high speeds. To date there has not been explicit experimental examination of the effect of external forcing on the dynamic behaviour of a fluid lubricated bearing, which requires a new purpose built rig.

In an earlier theoretical study, the dynamics of a gas lubricated bearing was analysed by Bailey *et al.* (2017) where a random external force is imposed on the rotor; modelled as a continuous, stationary, bounded process, with finite modes of frequencies in it spectrum. Utilising a Monte Carlo technique, a cumulative distribution function of the minimum gap was computed together with the evaluation of the minimum gap in reaching a prescribed tolerance.

In this work the dynamic response of the bearing is examined when the external force is more realistically described by a noise term; both white and coloured noise are considered. White noise is a limit of coloured noise (see e.g. Stratonovich (1968); Horsthemke & Lefever (1984); Hänggi & Jung (1995)), when the correlation time tends to zero and it can be a suitable model for external disturbances when the correlation time is very small. Coloured noise will result in a more representative model of the random forcing experienced by a bearing due to it having non-zero correlation time.

This paper outlines a model for a fluid lubricated bearing where the fluid flow through the bearing is coupled to the structural dynamics by the axial force of the fluid on the bearing face. An external force is imposed on the bearing rotor corresponding to modelling external disturbances as a noise term. This approach significantly differs from previous analysis of a gas-lubricated bearing operating under non-ideal conditions. Previously random forces with a discrete spectrum have been considered as in Bailey *et al.* (2017). In this work an external random force is described by a noise term with continuous spectrum. Advantages are that the

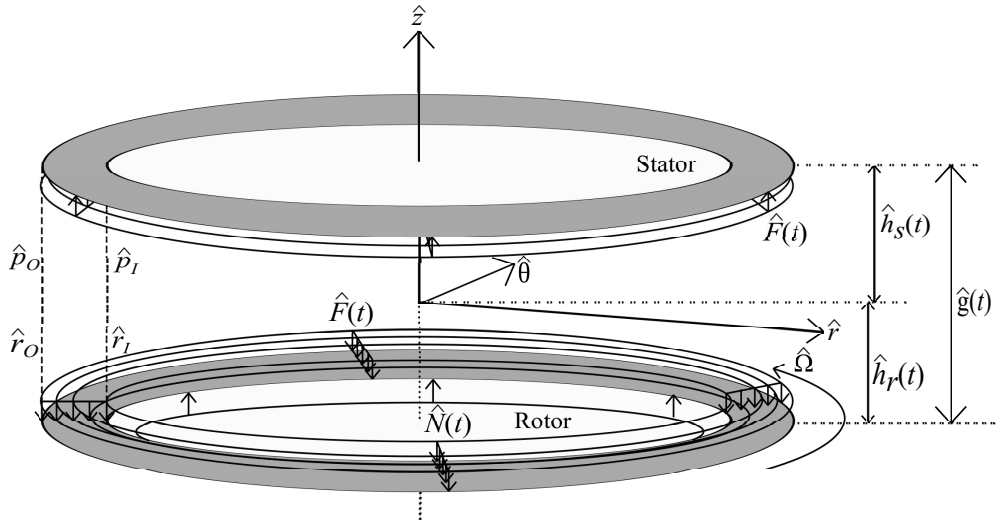

FIG. 2.1: Geometry and notation of a fluid lubricated bearing in radial coordinate system $(\hat{r},\hat{\theta},\hat{z})$, with stator height $\hat{h}_s(t)$, rotor height $\hat{h}_r(t)$, face clearance $\hat{g}(t)$, inner and outer radius denoted $\hat{r}_I$ and $\hat{r}_O$, respectively. Imposed pressure at inner and outer radius is given by $\hat{p}_I$ and $\hat{p}_O$, respectively and the rotor has angular rotation $\hat{\Omega}$. An external axial force $\hat{N}(t)$ is imposed on the rotor at $\hat{r}=\hat{r}_I$ and the axial fluid force on the bearing faces is denoted $\hat{F}(t)$ and occurs across the face radius.

corresponding noise is described more effectively by a limited number of parameters so can more robustly represent a given disturbance and is not restricted by the discretisation, thus can be better designed to replicate a specific disturbance for a given industrial application.

Key quantities of interest are the average time taken for the face clearance to reach a prescribed tolerance, together with its standard deviation; these give an indication of possible bearing failure. Additionally qualitative outcomes can inform evaluation of the average lifetime of a bearing configuration when it experiences external random disturbances. To infer parameters used in the derived models a purpose built research facility would be required; this forms part of our future work. The coupled governing equations are derived in Section 2 where a Reynolds equation for incompressible flow is coupled to spring-mass-damper systems representing axial rotor and stator displacements. An external force is imposed on the rotor, corresponding to either a white noise or coloured noise term. The resulting models take a form of stochastic differential equations (SDEs). Numerical techniques are formulated in Section 3 for both white and coloured noise, based on a simple random walk for the Dirichlet problem for linear parabolic partial differential equations, as developed by Milstein & Tretyakov (2002, 2004). Results of numerical experiments are presented in Section 4. Conclusions and discussion of the results are given in Section 5.

2 Mathematical model

A mathematical model is developed by retaining the key features of a fluid lubricated bearing with a simplified geometry as illustrated in Figure 2.1. A parallel rotor-stator configuration is defined in cylindrical polar coordinates following the approach by Bailey *et al.* (2013, 2017). The rotor and stator are modelled as a pair of coaxial axisymmetric annuli with inner and outer radius $\hat{r}_I$ and $\hat{r}_O$, respectively, and azimuthal angular rotation of the rotor $\hat{\Omega}$. External fluid pressures $\hat{p}_I$ and $\hat{p}_O$ are imposed at the inner and outer radius, respectively, allowing a pressure gradient to drive the radial flow. The axisymmetric face clearance is given by $\hat{g}(\hat{t}) = \hat{h}_s(\hat{t}) - \hat{h}_r(\hat{t})$, where $\hat{h}_s$ and $\hat{h}_r$ denote the stator and rotor axial displacements, respectively. The fluid exerts an axial force $\hat{F}(\hat{t})$ on the bearing faces and an external axial force $\hat{N}(\hat{t})$ is imposed on the rotor, modelling possible external destabilising behaviour, which is imposed at $\hat{r} = \hat{r}_I$.

A model for the fluid flow through the bearing is derived from the incompressible Navier-Stokes momentum and continuity equation; inertia effects are assumed to be negligible. The governing equations are expressed in dimensionless variables with dimensionless radius $r = \hat{r}/\hat{r}_0$, where $\hat{r}_0$ is taken to be a typical value of the bearing radius, and dimensionless height $z = \hat{z}/\hat{h}_0$, given a typical film thickness $\hat{h}_0$. Within a typical industrial application the aspect ratio is $\delta_0 = \hat{h}_0/\hat{r}_0 \ll 1$ which justifies the use of the lubrication approximation. The corresponding dimensionless velocities are taken as $(\hat{u}/\hat{U},\ \hat{v}/(\hat{\Omega}\hat{r}_0), \hat{w}/(\hat{h}_0\hat{T}^{-1}))$, with characteristic rotor velocity $\hat{\Omega}\hat{r}$ and time scale $\hat{T}$. A measure of the importance of the viscous time scale with kinematic viscosity ν is given by $\kappa = \hat{h}_0^2/\nu\hat{T}$ and is taken to be of $O(\delta_0)$, which results in the time scale $\hat{T} = O(\hat{h}_0\hat{r}_0/\nu)$. A corresponding pressure scale is taken as $P = \mu\hat{r}_0\hat{U}/\hat{h}_0^2$ to ensure the effects of viscosity are retained at leading order and the Reynolds number is $Re_U = \hat{U}\hat{h}_0/\nu$. The effects of gravity are neglected on taking $Re_U\delta_0 Fr^{-2} \ll 1$, where the Froude number $Fr = \hat{U}(\tilde{g}\hat{h}_0)^{-\frac{1}{2}}$ is assumed to be of $O(1)$; $\tilde{g}$ denotes the acceleration due to gravity.

The rotor and stator are solid surfaces, requiring no-normal flow and no-slip boundary condition to be imposed on the bearing faces. Although overall inertia effects are neglected, the rotor has rotational motion due to the azimuthal boundary condition. The resulting modified unsteady Reynolds equation is given by

$$\frac{dg}{dt} - \frac{Re_u\delta_0}{12\kappa r}\frac{\partial}{\partial r}\left(rg^3\frac{\partial p}{\partial r}\right) = 0, \tag{2.1}$$

with dimensionless face clearance $g = \hat{g}/\hat{h}_0$, see Bailey *et al.* (2013).

The modified Reynolds equation (2.1) can be solved directly, using pressure boundary conditions $p = p_I$ at $r = a$ and $p = p_O$ at $r = 1$, with $a = \hat{r}_I/\hat{r}_O$ being a measure of the inner radius. An explicit expression for the pressure field is given in Appendix A, equation (A.1), which can be integrated to give the fluid force on the bearing faces, F; see Appendix A, equation (A.2).

To formulate the structural equations, the stator and rotor are modelled as standard dimensionless spring-mass-damper systems

$$\begin{aligned}
\frac{d^2h_s}{dt^2} + D_a\frac{dh_s}{dt} + K_z\left(h_s - \frac{1}{2}\right) - \bar{\gamma}F\left(t, g, \frac{dg}{dt}\right) &= 0, \\
\frac{d^2h_r}{dt^2} + D_a\frac{dh_r}{dt} + K_z\left(h_r + \frac{1}{2}\right) + \bar{\gamma}F\left(t, g, \frac{dg}{dt}\right) &= \bar{\gamma}N(t),
\end{aligned} \tag{2.2}$$

based on the coordinate system shown in Figure 2.1 and the dimensionless rotor, stator axial displacements $h_{r,s} = \hat{h}_{r,s}/\hat{h}_0$. The dimensionless external force on the rotor is denoted by $N(t)$

and is imposed at $r = a$. Dimensionless damping, stiffness and force coupling parameter are given, respectively, by

$$D_a = \frac{\hat{D}_a \hat{T}}{\hat{m}}, \quad K_z = \frac{\hat{K}_z \hat{T}^2}{\hat{m}}, \quad \bar{\gamma} = \frac{\mu \hat{U} \hat{T}^2}{\hat{m} {\delta_0}^3}, \tag{2.3}$$

where $\hat{m}$ is a relevant bearing mass, and $\hat{D}_a$ and $\hat{K}_z$ are the dimensional damping and stiffness parameters, respectively.

The structural equations (2.2) are coupled to the modified Reynolds equation (2.1) through the axial force of the fluid on the bearing faces. This results in a second order ordinary differential equation for the face clearance of the form

$$\frac{d^2 g}{dt^2} + \left(D_a + \frac{2\bar{\gamma} B}{g^3} \right) \frac{dg}{dt} + K_z \, (g - 1) - 2\bar{\gamma} A = -\bar{\gamma} N(t), \tag{2.4}$$

with the initial condition

$$g(0) = g_0, \qquad \frac{dg}{dt}(0) = z_0.$$

Note that the coefficient $2\bar{\gamma} B / g^3$ has a singularity when the face clearance $g \to 0$.

It is convenient to write equation (2.4) as a system of first order differential equations

$$\frac{dg}{dt} = z, \qquad \frac{dz}{dt} = -\left(D_a + \frac{\bar{B}}{g^3} \right) z - K_z (g - \bar{A}) - \frac{\gamma}{2} N(t), \tag{2.5}$$

with $\bar{B} = \gamma B$, $\bar{A} = 1 + \gamma A / K_z$ and rescaled force coupling parameter $\gamma = 2\bar{\gamma}$.

The external force $N(t)$ on the rotor models the effect of external excitations on the bearing, which arise from the composite system in which the bearing is placed. The lack of precise knowledge about the external force imposed on the bearing system is reflected by considering $N(t)$ as a noise term. Consideration of the time scales of the noise and physical system are discussed by Hänggi & Jung (1995). The noise term should have a well-defined characteristic (correlation) time, which motivates choosing coloured noise for modelling $N(t)$. The time scale of the noise depends on the characteristic response time of the bearing system $\hat{T}$; the correlation time of $N(t)$ in the model should be comparable to or much larger than the characteristic time of the bearing system to relax, i.e. correlation times should be of order $O(\delta_0)$ or larger. The noise term can be considered to represent cumulative effects of many weakly coupled environmental degrees of freedom. For example, the bearing may experience disturbances due to vibrations, from other components within the larger system and due to contaminants. A limiting case is that of white noise, which can be viewed as a limit of coloured noise when its correlation length appropriately tends to zero (see Stratonovich (1968); Hänggi & Jung (1995)). This limiting case is mathematically simpler to analyse and is introduced first (Section 2.1) followed by the case of coloured noise (Section 2.2).

2.1 *Response to white noise*

The external force $N(t)$ in (2.5) is taken as a Gaussian white noise with an expected value $E[N(t)] = 0$ and covariance $E[N(t)N(s)] = \bar{\sigma}^2 \delta(t - s)$, where $\bar{\sigma}$ is a noise intensity parameter.

For the case of white noise, equation (2.5) can be formulated in the differential form

$$\begin{aligned} dg &= z dt, & g(s) &= g_0 > 0, \\ dz &= -\left(\left(D_a + \frac{\bar{B}}{g^3}\right) z + K_z(g - \bar{A})\right) dt + \sigma dw(t), & z(s) &= z_0. \end{aligned} \tag{2.6}$$

In (2.6) $w(t)$ is a standard Wiener process defined on a filtered probability space $(\Omega, \mathcal{F}, \mathcal{F}_t, P)$ with a scaled noise intensity parameter $\sigma = \gamma\bar{\sigma}/2$. The associated notation for the solution of (2.6) is $g(t) = g_{s,g_0,z_0}(t)$, $z(t) = z_{s,g_0,z_0}(t)$, $t \geqslant s$, where $g(s) = g_0$, $z(s) = z_0$ are the initial conditions at $t = s$; if $s = 0$, for compactness we write $g_{g_0,z_0}(t)$, $z_{g_0,z_0}(t)$ instead of $g_{0,g_0,z_0}(t)$, $z_{0,g_0,z_0}(t)$, $t \geqslant 0$. Existence and uniqueness of the solution to (2.6), as well as boundedness of its moments, are provided in Appendix B. This analysis also establishes formally that $g_{g_0,z_0}(t)$ can never reach zero, resulting in a positive face clearance always, although it may become arbitrary small.

Of interest is the time when the face clearance $g(t)$ first reaches a given small tolerance, $\delta > 0$. To define this time, it is convenient to introduce a space domain $G^\delta = (\delta, \infty) \times \mathbf{R}$, i.e. a domain where the face clearance $g(t)$ is larger than δ and the velocity $z(t)$ can take any real number. We also define the time-space domain $Q^\delta = [0, T) \times G^\delta$. We denote θ^δ to be the first exit time of the trajectory $(g_{s,g_0,z_0}(t),\, z_{s,g_0,z_0}(t))$, $t \geqslant s$, from the domain G^δ, i.e.,

$$\theta^\delta = \theta^\delta_{s,g_0,z_0} = \inf\{t : g_{s,g_0,z_0}(t) = \delta\},$$

as the first time when $g_{s,g_0,z_0}(t)$ reaches δ, i.e. the time at which the face clearance first becomes as small as the tolerance. We also define $\tau^\delta = \theta^\delta \wedge T$, which is the first exit time of the space-time trajectory $(t, g_{s,g_0,z_0}(t), z_{s,g_0,z_0}(t))$ from the domain Q^δ, i.e. τ^δ takes the value of the time at which the bearing face clearance first reaches the prescribed tolerance δ or T if the face clearance does not reach the tolerance in the time period examined.

For an initial condition (s, g_0, z_0), the expectation of a quantity of interest can be expressed as

$$u(s, g_0, z_0) := E\left[\varphi(g_{s,g_0,z_0}(\tau^\delta_{s,g_0,z_0})) + \int_s^{\tau^\delta_{s,g_0,z_0}} f(t, g_{s,g_0,z_0}(t))dt\right], \tag{2.7}$$

for some functions φ and f; these functions depend on the quantity of interest and are discussed below. The function $u(s, g, z)$ satisfies the backward Kolmogorov equation with Dirichlet boundary condition (i.e., the Dirichlet problem for the linear parabolic PDE with negative direction of time; see e.g. R. Z. Hasminskii (1980); Freidlin (1985); Milstein & Tretyakov (2004):

$$\begin{aligned} \frac{\partial u}{\partial s} + \frac{\sigma^2}{2}\frac{\partial^2 u}{\partial z^2} - \left(\left(D_a + \frac{\bar{B}}{g^3}\right) z + K_z(g - \bar{A})\right)\frac{\partial u}{\partial z} + z\frac{\partial u}{\partial g} + f(s, g) &= 0,\ (s, g, z) \in Q^\delta, \\ u(T, g, z) &= \varphi_1(g),\ (g, z) \in \bar{G}^\delta, \\ u(s, \delta, z) &= \varphi_2(s),\ s \leqslant T,\ z \in \mathbf{R}, \end{aligned} \tag{2.8}$$

where φ_1 and φ_2 are related to φ in (2.7) so that

$$\varphi(g(\tau^\delta)) = \begin{cases} \varphi_1(g(T)), & \text{if } \theta^\delta > T, \\ \varphi_2(\theta^\delta), & \text{otherwise.} \end{cases} \tag{2.9}$$

The probabilistic representation (2.7), (2.6) of the solution to the PDE problem (2.8)-(2.9) is often called the Feynman-Kac formula or averaging-over-characteristics formula.

As mentioned previously, the functions f, φ_1 and φ_2 can be chosen to examine particular quantities of interest. To find the probability that the face clearance reaches the given tolerance before time T requires $f = 0,\ \varphi_1(g) = 0,\ \varphi_2(t) = 1$ resulting in $u(0,g,z) = P(\tau^\delta_{0,g,z} < T) = P(\theta^\delta_{0,g,z} < T)$. Similarly, the first and second moments of the first exit time, τ^δ, are given by $u(0,g,z) = E[\tau^\delta]$ and $u(0,g,z) = E[\tau^\delta]^2$, respectively, and can be found using $\varphi_1(g) = 0$, $\varphi_2(s) = 0$ and $f = 1$ or $f = 2s$, respectively.

Noting that from the applicable point of view at the initial time $s = 0$, the gap g_0 and velocity z_0 should be considered as uncertain, we model the initial condition $g_0,\ z_0$ as independent random variables. In the following we choose g_0 as a truncated normal random variable, to ensure its positivity, and z_0 as a normal random variable; it is noted that these random variables are independent of the Wiener process $w(t),\ t \geqslant 0$. The quantities of interest can then be expressed as

$$U := E\left[\varphi(g_{g_0,z_0}(\tau^\delta_{g_0,z_0})) + \int_0^{\tau^\delta_{g_0,z_0}} f(t, g_{g_0,z_0}(t))dt\right] \tag{2.10}$$

$$= E[u(0,g_0,z_0)]. \tag{2.11}$$

In (2.10) the expectation is taken over the trajectories $(g_{g_0,z_0}(t), z_{g_0,z_0}(t))$, $t \geqslant 0$ and random initial condition (g_0, z_0), whereas in (2.11) the expectation is taken over the initial condition (g_0, z_0) only.

2.2 *Response to coloured noise*

The external force $N(t)$ in (2.5) is modelled as coloured noise, using the Ornstein-Uhlenbeck process, giving the following system of SDEs (see, e.g. Horsthemke & Lefever (1984); Hänggi & Jung (1995); Milstein & Tretyakov (2004)):

$$\begin{aligned} dg &= z dt, & g(0) &= g_0, \\ dz &= -\left(\left(D_a + \frac{\bar{B}}{g^3}\right) z + K_z(g - \bar{A})\right) dt + \sigma y dt, & z(0) &= z_0, \\ dy &= \alpha(-y dt + dw), & y(0) &= y_0, \end{aligned} \tag{2.12}$$

where $\alpha > 0$ is a constant and the remaining notation is as in (2.6). Existence and uniqueness of the solution to (2.12) can be proved similar to the white noise case (see Appendix B); the corresponding proof is omitted here. In particular, as in the white noise case, here the bearing gap $g_{g_0,z_0,y_0}(t)$ remains positive always, although it may become arbitrary small.

The coloured noise $y(t)$ is a Gaussian process with the properties

$$E[y(t)] = y_0 e^{-\alpha t} \qquad \text{and} \qquad E[y(t)y(s)] = \frac{\alpha}{2} e^{-\alpha|t-s|} + \left({y_0}^2 - \frac{\alpha}{2}\right) e^{-\alpha(t+s)}. \tag{2.13}$$

We note that the Ornstein-Uhlenbeck process $y(t)$ is ergodic with the invariant measure $\varrho_y(x) = (\pi\alpha)^{-1/2} e^{-x^2/\alpha}$. In order for the noise term $N(t)$ in (2.5) to be a stationary process (the natural requirement for a model of external disturbances), the initial condition y_0 in (2.12) is chosen

to be a random variable distributed according to the invariant measure $\varrho_y(x)$. The Lorentzian power spectrum of the coloured noise is

$$S_y(\omega) = \frac{\alpha^2}{\alpha^2\omega^2 + 1},$$

i.e. the coloured noise has a characteristic range of frequencies. Depending upon the industrial application of the bearing, the parameters can be chosen such that the power spectrum is representative of the disturbances experienced by the bearing. This property of coloured noise is in contrast to that of white noise, where the power spectrum is flat for all $\omega \in \mathbf{R}$.

The characteristic correlation time (time scale) of the noise in (2.12) is given by $1/\alpha$. When $\alpha \to \infty$ (i.e. the correlation time $1/\alpha$ goes to zero), the correlation function of $y(t)$ (see (2.13)) tends to the Dirac delta function and the power spectrum becomes flat. In this limit coloured noise converges weakly to the white noise, see e.g. Stratonovich (1968); Horsthemke & Lefever (1984); Hänggi & Jung (1995).

REMARK 2.1 We note the coloured noise used here can be generalised by replacing $y(t)$ in (2.12) with a collection of $y_i(t)$ each with a different characteristic correlation time $1/\alpha_i$.

Introduce the space domain $G^\delta = (\delta, \infty) \times \mathbf{R}^2$ and the time-space domain $Q^\delta = [0, T) \times G^\delta$. Let θ^δ be the first exit time of the trajectory $(g_{s,g_0,z_0,y_0}(t),\ z_{s,g_0,z_0,y_0}(t), y_{s,y_0}(t))$, $t \geqslant s$, from the domain G^δ, i.e.,

$$\theta^\delta = \theta^\delta_{s,g_0,z_0,y_0} = \inf\{t : g_{s,g_0,z_0,y_0}(t) = \delta\},$$

(here y_0 is deterministic). We also define $\tau^\delta = \theta^\delta \wedge T$, which is the first exit time of the space-time trajectory $(t, g_{s,g_0,z_0,y_0}(t),\ z_{s,g_0,z_0,y_0}(t), y_{s,y_0}(t))$ from the domain Q^δ, i.e. τ^δ takes the value of the time at which the bearing face clearance first reaches the prescribed tolerance δ or T if the face clearance does not reach the tolerance in the time period examined. Similarly to (2.7), consider the expectation for some functions φ and f:

$$u(s, g_0, z_0, y_0) := E\left[\varphi(g_{s,g_0,z_0,y_0}(\tau^\delta_{s,g_0,z_0,y_0})) + \int_s^{\tau^\delta_{s,g_0,z_0,y_0}} f(t, g_{s,g_0,z_0,y_0}(t))dt\right]. \tag{2.14}$$

The expectation $u(s, g, z, y)$ satisfies the backward Kolmogorov equation

$$\begin{aligned} \frac{\partial u}{\partial s} + \frac{\alpha^2}{2}\frac{\partial^2 u}{\partial y^2} - \left(\left(D_a + \frac{\bar{B}}{g^3}\right)z + K_z(g - \bar{A})\right)\frac{\partial u}{\partial z} + z\frac{\partial u}{\partial g} - \alpha y\frac{\partial u}{\partial y} + f(s,g) &= 0,\ (s,g,z,y) \in Q^\delta, \\ u(T, g, z, y) = \varphi_1(g), &\quad x \geqslant \delta,\ z, y \in \mathbf{R}, \\ u(s, \delta, z, y) = \varphi_2(s), &\quad s \leqslant T,\ z, y \in \mathbf{R}. \end{aligned} \tag{2.15}$$

For the quantities of interest, y_0 is random and distributed according to the invariant measure $\varrho_y(x)$ of $y(t)$. As in the white noise case, we model the initial conditions g_0, z_0 as independent random variables which are independent of y_0; the random variables g_0, z_0 and y_0 are independent of the Wiener process $w(t)$, $t \geqslant 0$. As previously we choose g_0 as a truncated normal random variable and z_0 as a normal random variable. Then, analogous to (2.16), we

introduce the expectation

$$U := E\left[\varphi(g_{g_0,z_0,y_0}(\tau^{\delta}_{g_0,z_0,y_0})) + \int_s^{\tau^{\delta}_{g_0,z_0,y_0}} f(t, g_{g_0,z_0,y_0}(t))dt\right]$$
$$= E[u(0,g_0,z_0,y_0)]. \tag{2.16}$$

3 Numerical method

To evaluate quantities of interest U, either from (2.10)-(2.11) (the white noise case) or (2.16) (the coloured noise case), we use the Monte Carlo technique together with approximation of the SDEs (2.6) (the white noise case) or (2.12) (the coloured noise case). To simulate the SDEs in bounded domains, we exploit the simplest random walk for the Dirichlet problem. Following Milstein & Tretyakov (2002, 2004), we present in Section 3.1 the white noise case and in Section 3.2 the coloured noise case.

We simulate the SDEs on a time interval $[0,T]$, which we uniformly discretise with a time step $\triangle T > 0$; correspondingly $\bar{N} = T/\triangle T$ is the maximum possible number of time steps per discrete trajectory in the algorithms presented below and $t_{k+1} = t_k + \triangle T$, $k = 0, \ldots, \bar{N} - 1$.

Instead of the exact trajectories of (2.6) (the white noise case) or (2.12) (the coloured noise case) in the expectations (2.11) or (2.16), respectively, we substitute their discrete approximations obtained by the algorithms presented below and thus we obtain an approximation $\bar{U}$ of U. The difference $\bar{U} - U$ is the weak-sense error of these algorithms (see Milstein & Tretyakov (2004)) which is of order one, i.e.

$$|\bar{U} - U| \leqslant C \triangle T, \tag{3.1}$$

where $C > 0$ is a constant independent of $\triangle T$.

To compute the expectation $\bar{U}$, we exploit the Monte Carlo technique; we run a large but finite number M of independent discrete approximate trajectories and find the corresponding sample mean $\hat{U}$, which approximates $\bar{U}$, as well as the corresponding sample variance $\hat{V}$. The statistical (Monte Carlo) error $\bar{U} - \hat{U}$ is quantified by $R_{mc} = \sqrt{\hat{V}}/\sqrt{M}$ so that $\bar{U}$ belongs to the confidence interval (see, e.g. Milstein & Tretyakov (2004)):

$$\bar{U} \in \left(\hat{U} - 2R_{mc}, \hat{U} + 2R_{mc}\right) \tag{3.2}$$

with probability 0.95.

The simulated quantities $\hat{U}$ are subjected to two errors: (i) the bias which is equal to $\bar{U} - U$, and the size of which is controlled by choosing a sufficiently small time step $\triangle T$; and (ii) the statistical error which is controlled by choosing a sufficiently large number M of independent realisations.

3.1 *White noise*

Applying the weak Euler approximation with the simplest simulation of noise (see Milstein & Tretyakov (2004)) to the system (2.6) with a given initial condition $(g_0, z_0) \in G$ at $t = 0$ gives

$$z_{k+1} = z_k - \left(\left(D_a + \frac{\bar{B}}{{g_k}^3}\right) z_k + K_z(g_k - \bar{A})\right) \triangle T - \sigma\sqrt{\triangle T}\,\xi_k,$$
$$g_{k+1} = g_k + z_{k+1} \triangle T, \tag{3.3}$$

where ξ_k are mutually independent random variables taking values ± 1 with probability 1/2. A Markov chain (t_k, g_k, z_k) is constructed to approximate $(t_k, g(t_k), z(t_k))$, where $(g(t), z(t))$ is the solution of (2.6), as described in the following algorithm.

Algorithm 3.1 *White noise case: algorithm for simulating a trajectory* (t_k, g_k, z_k).

Step 1 Sample the initial condition g_0, z_0. Set $k = 0$.

Step 2 Sample ξ_k and compute z_{k+1}, g_{k+1} according to (3.3).

Step 3 If $g_{k+1} > \delta$ and $k < \bar{N} - 1$ then set $k = k + 1$ and go to Step 2; otherwise go to Step 4.

Step 4 If $g_{k+1} \leqslant \delta$ then set $\varkappa = k$, $g_\varkappa = g_k$ and $z_\varkappa = z_k$ and exit the algorithm; otherwise go to Step 5.

Step 5 Set $\varkappa = \bar{N}$, $g_\varkappa = g_{\bar{N}}$ and $z_\varkappa = z_{\bar{N}}$ and exit the algorithm.

It is noted that $t_\varkappa$ obtained in the algorithm approximates the stopping time τ^δ. The algorithm (or in other words, discrete trajectory) stops when either the integration time reaches the end of the time interval T or the approximate trajectory escapes from the domain G. Applying similar arguments to those used in Milstein & Tretyakov (2002, 2004), it can be proved that this algorithm is of first weak order (see equation (3.1)).

3.2 *Coloured noise*

To simulate the system of equations (2.12), the linear equation for $y(t)$ is solved exactly and a weak Euler approximation is applied to the other two equations in the system; this gives iterative values

$$\begin{aligned} y_{k+1} &= e^{-\alpha \triangle T}\,(y_k + \alpha \eta_k)\,, \\ z_{k+1} &= z_k - \left(\left(D_a + \frac{\bar{B}}{{g_k}^3} \right) z_k + K_z (g_k - \bar{A}) + \sigma y_{k+1} \right) \triangle T, \\ g_{k+1} &= g_k + z_{k+1} \triangle T, \end{aligned} \tag{3.4}$$

where η_k are mutually independent Gaussian random variables with zero mean and variance $(e^{2\alpha \triangle T} - 1)/2\alpha$. A Markov chain (t_k, g_k, z_k, y_k) is constructed to approximate $(t_k, g(t_k), z(t_k), y(t_k))$, where $(g(t), z(t), y(t))$ is the solution of (2.12) analogously to Algorithm 3.1.

Algorithm 3.2 *Coloured noise case: algorithm for simulating a trajectory* (t_k, g_k, z_k, y_k).

Step 1 Sample the initial condition g_0, z_0, y_0. Set $k = 0$.

Step 2 Sample η_k and compute y_{k+1}, z_{k+1}, g_{k+1} according to (3.4).

Step 3 If $g_{k+1} > \delta$ and $k < \bar{N} - 1$ then set $k = k + 1$ and go to Step 2; otherwise go to Step 4.

Step 4 If $g_{k+1} \leqslant \delta$ then set $\varkappa = k$, $g_\varkappa = g_k$, $z_\varkappa = z_k$, and $y_\varkappa = y_k$ and exit the algorithm; otherwise go to Step 5.

Step 5 Set $\varkappa = \bar{N}$, $g_\varkappa = g_{\bar{N}}$, $z_\varkappa = z_{\bar{N}}$, and $y_\varkappa = y_{\bar{N}}$ and exit the algorithm.

This algorithm is of first weak order.

4 Numerical experiments

Results are given for a fixed bearing configuration, with the following dimensionless parameters calculated using the scalings in Section 2 from dimensional parameters which are chosen to be representative of a feasible industrial configuration for a gas turbine application. The bearing has a narrow annulus $a = 0.8$, with ambient pressure imposed at the inner and outer radius $p_a = p_I = p_O = 1$ and structural stiffness and damping parameters taken to be $K_z = 55.56$ and $D_a = 1$, respectively. The unscaled noise intensity parameter takes the value $\bar{\sigma} = 20$, the non-dimensional parameter $\eta = 4.5$ and prescribed tolerance of g is given by $\delta = 0.05$. The time horizon for studying the bearing is taken as $T = 1000$; this is assumed to be the maximum time that a bearing will experience an individual disturbance. We note that if the mean time $E\tau^\delta$ is equal to $T = 1000$ then the minimum gap does not reach the prescribed tolerance for the given conditions with probability one.

A time step of $\triangle t = 1\text{x}10^{-5}$ is used as this is sufficiently small to give a solution of the required accuracy and, in particular, to have the numerical integration error not exceeding the Monte Carlo error. Indeed, for example for $\gamma = 10$ and $\alpha = 100$, we obtained the following results for the average first exit time $E\tau^\delta$ computed with different time steps: $\triangle t = 0.125 \times 10^{-3}$ – $E\tau^\delta \doteq 3.19 \pm 0.12$, $\triangle t = 1 \times 10^{-4}$ – $E\tau^\delta \doteq 3.15 \pm 0.12$, $\triangle t = 0.5 \times 10^{-4}$ – $E\tau^\delta \doteq 3.03 \pm 0.12$; $\triangle t = 1 \times 10^{-5}$ – $E\tau^\delta \doteq 2.92 \pm 0.11$, and $\triangle t = 1 \times 10^{-6}$ – $E\tau^\delta \doteq 2.97 \pm 0.12$. The numbers after $\pm$ give the Monte Carlo error. These results confirm that our choice of $\triangle t = 1\text{x}10^{-5}$ is sufficient. The number of independent discrete approximate trajectories M are chosen so that the Monte Carlo error is less than 5.5%, giving a comprise between computational time and accuracy. The initial condition g_0 is sampled from a truncated normal distribution, which is obtained from normal distribution with mean 1 and standard deviation 0.5, and the lower truncation bound is $g_a = 0.1$ and the upper truncation bound is $g_b = 2$. These bounds are chosen due to the geometric restrictions limiting the maximum value of the face clearance and the minimum value is assumed to be larger than the prescribed tolerance. The initial condition z_0 is sampled from normal distribution with mean -1 and standard deviation 0.5 as it is assumed that the faces are initially forced towards each other. Parameters of the model could be inferred from a purpose built research facility; this work is currently ongoing. The deterministic bearing parameters would be given as the equivalent nondimensional values of those of the research facility, found using the scalings in Section 2. The initial condition distribution of g_0 could be estimated from direct measurements of the face clearance over a sufficiently long period of time, and the equivalent distribution for z_0 can be inferred from this data using the corresponding time period.

Initially the effect of imposing an external white noise term on the rotor is examined. In particular, we are interested in how the average time for the face clearance to reach the tolerance depends on the coupling parameter γ.

Figure 4.1 shows the average time for the minimum gap to reach the given tolerance $\delta = 0.05$ against increasing values of the force coupling parameter γ. The error bars give the Monte Carlo error and the dashed lines denote one standard deviation above and below the mean value. Taking the case of force coupling parameter $\gamma = 1$, the average time at which the face clearance reaches the prescribed tolerance is $E\tau^\delta \approx 14.4 \pm 0.704$. Increasing the force coupling parameter to $\gamma = 6$ gives the average time at which the face clearance reaches the prescribed tolerance decreasing to $E\tau^\delta \approx 2.84 \pm 0.129$. Increasing the force coupling parameter further to $\gamma = 10$ results in similar average times for the face clearance reaching the prescribed tolerance.

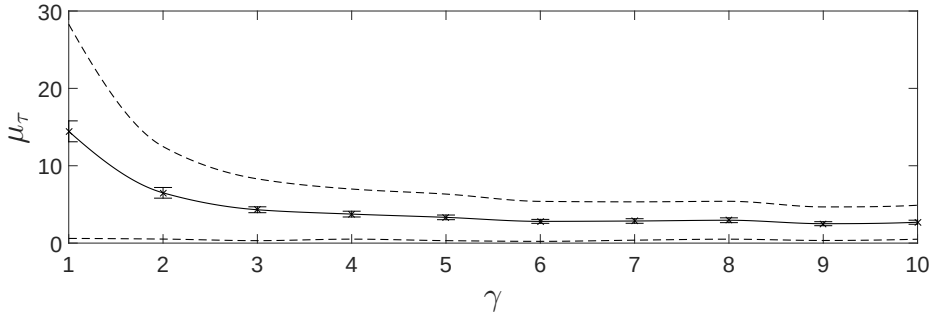

FIG. 4.1: Mean time $E\tau^\delta$ for the minimum gap to reach a prescribed tolerance $\delta = 0.05$ against force coupling parameter γ in the case of white noise; error bars give the Monte Carlo error bounds and dashed lines denote one standard deviation from the mean.

During the bearing operation, the bearing characteristics may be modified over time as a result of the disturbances, leading to the values for the bearing parameters no longer being a true representation of the system. Therefore, for a bearing configuration with force coupling parameter $\gamma > 6$, the bearing performance should be maintained even if factors affecting the force coupling parameter are modified during operation. For bearing configurations with a smaller force coupling parameter, there may be a significant change in the average time taken for the face clearance to reach the predicted tolerance, which in turn may lead to unpredicted face contact.

For the case of coloured noise, Figure 4.2 shows the average time taken for the face clearance to reach the prescribed tolerance; corresponding to values of the coloured noise parameter $\alpha = 1$, $\alpha = 10$, $\alpha = 20$ and $\alpha = 100$, and for increasing value of the force coupling parameter γ. Selecting the coloured noise parameter $\alpha = 1$ and force coupling parameter $\gamma = 1$, the face clearance does not reach the prescribed tolerance since $E\tau^\delta \approx 1000 \pm 1.82\text{x}10^{-13}$, which is the time period over which the dynamic behaviour of the bearing is examined. Increasing the parameter describing the force coupling gives the face clearance reaching the prescribed tolerance; initially there is a sharp decrease in the average time at which the face clearance reaches the prescribed tolerance, resulting in $E\tau^\delta \approx 82.7 \pm 4.09$ for $\gamma = 4$, before having a smaller decrease leading to $E\tau^\delta \approx 19.0 \pm 0.950$ at $\gamma = 10$. Results predict for a small coloured noise parameter $\alpha = 1$ and force coupling parameter $\gamma = 1$ a minimum gap larger than $g = 0.05$ is maintained over the time examined, however an increase in γ results in the prescribed gap being reached. Thus, a small increase in the force coupling parameter from $\gamma = 1$ may lead to premature face contact and possible bearing failure.

Increasing the coloured noise parameter α gives the face clearance reaching the prescribed tolerance for all values of the force coupling parameter γ, and with a smaller average time $E\tau^\delta$. For small values of the force coupling parameter, there are large decreases in the average time, otherwise there are smaller decreases. Increasing the coloured noise parameter α (i.e., the inverse of the characteristic correlation time of the noise) gives the average time at which the face clearance reaches the prescribed tolerance $E\tau^\delta$; these tend to the value of that obtained for white noise, see Table 4.1, which is expected since as $\alpha \to \infty$ the coloured noise tends to the

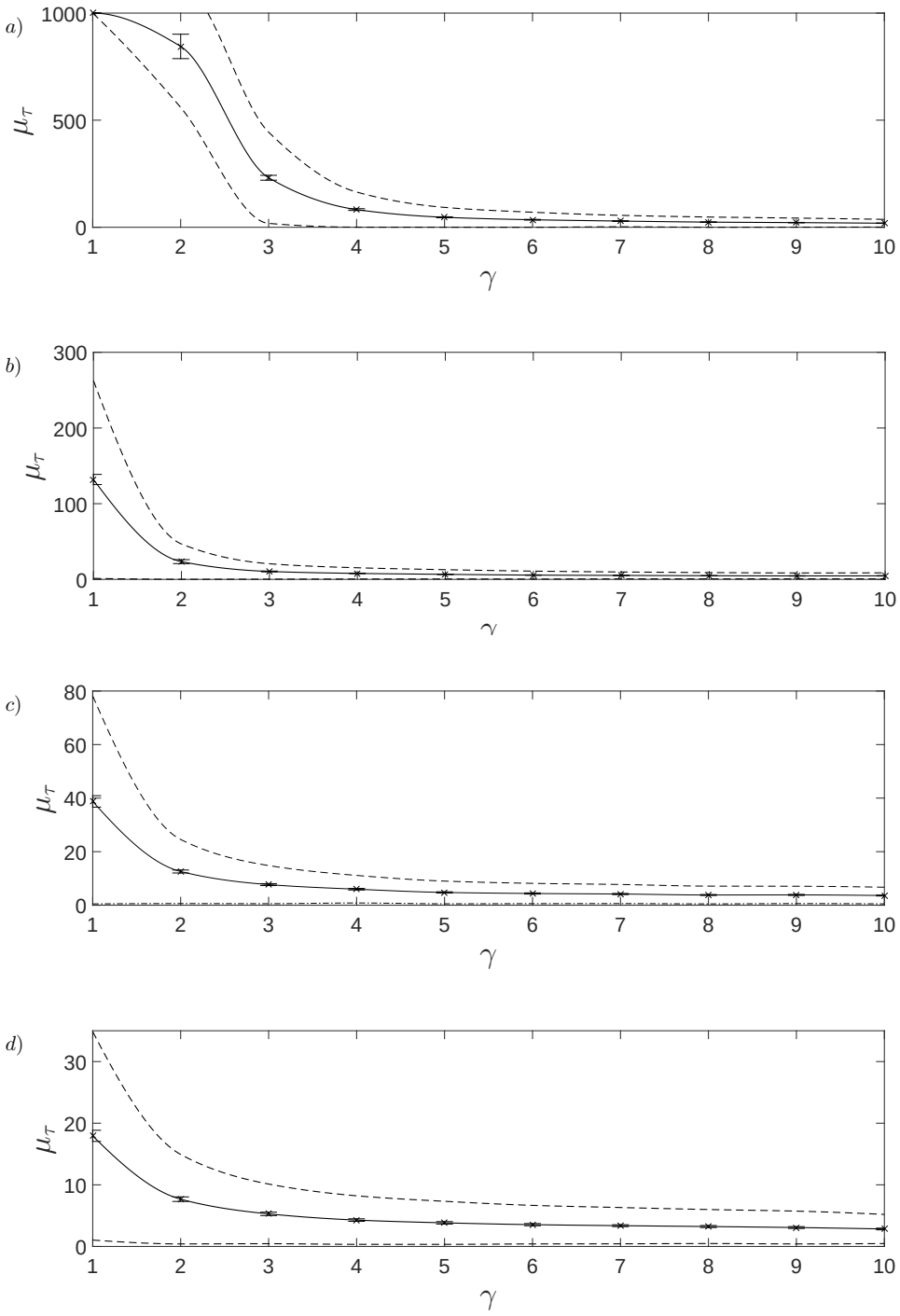

FIG. 4.2: Mean time $E\tau^\delta$ for the minimum gap to reach the prescribed tolerance $\delta = 0.05$ against force coupling parameter γ in the case of coloured noise with the parameter a) $\alpha = 1$, b) $\alpha = 10$, c) $\alpha = 20$ and d) $\alpha = 100$; error bars give the Monte Carlo error and dashed lines denote one standard deviation from the mean.

white noise.

Table 4.1: Average time $E\tau^{\delta}$ for the face clearance to reach tolerance $\delta = 0.05$ for force coupling parameter $1 \leqslant \gamma \leqslant 10$ in the case of coloured noise $1 \leqslant \alpha \leqslant 100$ and white noise.

	coloured noise				white noise
	$\alpha = 1$	$\alpha = 10$	$\alpha = 20$	$\alpha = 100$	
$\gamma = 1$	$1000 \pm 1.83\text{x}10^{13}$	132 ± 6.72	38.6 ± 2.14	17.9 ± 0.904	14.4 ± 0.704
$\gamma = 4$	82.7 ± 4.09	7.90 ± 0.413	5.98 ± 0.295	4.28 ± 0.203	3.50 ± 0.173
$\gamma = 6$	35.2 ± 1.68	5.64 ± 0.289	4.38 ± 0.214	3.54 ± 0.177	2.84 ± 0.129
$\gamma = 10$	19.0 ± 0.950	4.66 ± 0.235	3.62 ± 0.176	2.83 ± 0.139	2.60 ± 0.123

Results show the coloured noise parameter α has a large effects on predictions of a bearing life time, i.e. the average length of time before the prescribed minimum gap between the bearing faces is reached, $E\tau^{\delta}$. Thus, to obtain accurate predications it is necessary to precisely describe the external disturbances on the bearing. If the bearing characteristics are amended during operation as a result of the external disturbances, the force coupling parameter value may no longer be a true representation of the system, and the predicted results may no longer be accurate. For suitably large values of the force coupling parameter, a small change results in associated small changes in predicted average time for the face clearance to reach the prescribed tolerance; in contrast to cases with small force coupling parameters. Therefore, a desirable feature in a bearing configuration will have as large a force coupling parameter as possible. We note that in this work we take into account uncertainties caused by environmental random fluctuations which are naturally modelled as an additive noise. To account for bearing characteristics that can randomly change over time, the corresponding parameters can additionally be modelled as random processes resulting in multiplicative noises. Noting changes of the bearing characteristics are generally much slower than environmental fluctuations, this aspect is neglected in this paper.

5 Conclusions

A dynamical model for a fluid lubricated bearing is derived, where the axial rotor and stator displacements are modelled by spring-mass-damper systems. The fluid flow through the bearing is described by a Reynolds equation for incompressible flow and coupled to the bearing via the axial force from the fluid on the bearing faces. To evaluate the bearing dynamics when the system experiences typical external disturbances, an external force is imposed on the rotor, which is modelled by a noise term. A key quantity of interest is the average time taken for the face clearance to reach a prescribed tolerance; typically a small value where the size of the face clearance could lead to possible face contact and potential bearing failure. Predictions could enable more accurate average lifetime of a bearing to be identified when experiencing external random disturbances.

To compute the average time at which the prescribed tolerance is reached before a fixed time horizon, a numerical technique is implemented using Monte Carlo techniques and a simple random walk for Dirichlet problems following Milstein & Tretyakov (2002, 2004). Results for the case of coloured noise show that increasing the force coupling parameter decreases the average time at which the face clearance reaches the prescribed tolerance. As the characteristic

correlation time $1/\alpha$ of coloured noise decreases, the average time of the face clearance reaching the prescribed tolerance decreases. For very small values of $1/\alpha$, the average time tends to the value for white noise, as expected.

This work identifies the average time for the minimum gap to reach a prescribed tolerance between the bearing faces which is dependent on the coloured noise parameter α. Results show that it is necessary to accurately describe the external disturbances on the bearing for the given industrial application to obtain meaningful predications. The outcomes suggest that to attain a robust dynamic bearing, the design should be such that a small change in the value of the force coupling parameter has a limited effect on the average time for the bearing gap to reach the prescribed tolerance.

Acknowledgement

This work was supported by funding from the EPSRC Doctoral Prize grant No. EP/M506588/1.

A Derivation of an explicit expression for the pressure field

An explicit expression for the pressure field is given by

$$p(t,g,g') = p_O + (p_I - p_O)\frac{\ln r}{\ln a} + \frac{dg}{dt}\frac{\kappa}{4g^3 Re_u \delta_0}\left(r^2 - 1 + (1-a^2)\frac{\ln r}{\ln a}\right), \tag{A.1}$$

which is obtained from integration of the modified Reynolds equations (2.1). The corresponding fluid force on the bearing faces is then

$$F(t,g,g') \quad = \quad 2\pi\int_a^1 (p-p_a) r dr = A - \frac{B}{g^3}\frac{dg}{dt}, \tag{A.2}$$

with

$$\begin{aligned} A &= \pi\left(p_O - p_a - (p_I - p_a)a^2 - \frac{(1-a^2)(p_I - p_O)}{2\ln a}\right), \\ B &= \eta\pi\left(1 - a^4 + \frac{(1-a^2)^2}{\ln a}\right), \end{aligned} \tag{A.3}$$

where $\eta = 3\kappa/2Re_u\delta_0$.

B White noise case: Existence and uniqueness of the solution

In this section we prove existence and uniqueness of the solution to (2.6) for all $t \geqslant 0$ as well as boundedness of its moments. The proof is based on making use of Lyapunov functions (see R. Z. Hasminskii (1980)). The model (2.6) is well-posed for the considered engineering problem only if the solution $(g_{g_0,z_0}(t), z_{g_0,z_0}(t)) \in G^0$, $(g_0,z_0) \in G^0$, for all $t \geqslant 0$ or, in other words, the solution is regular: the stopping time $\theta^*_{g_0,z_0} = \inf\{t : (g(t),z(t)) \notin G^0\}$ of the process $(g(t),z(t))$ to either explode or $g(t)$ reaching 0 is such that

$$P(\theta^*_{g_0,z_0} = \infty) = 1. \tag{B.1}$$

Thus, the gap $g(t)$ cannot become zero in finite time; this would lead to a blow-up of the right-hand side of (2.6) due to the cubic singularity at 0 and neither $g(t)$ and $z(t)$ can satisfy the resulting equation. To this end, we prove the following proposition.

Proposition 1. *Given an initial condition* (g_0, z_0) *at* $t = 0$ *with* $g_0 > 0$ *and* $z_0 \in \mathbf{R}$*, there exists a unique solution* $(g(t), z(t))$ *of the SDEs (2.6) for any* $t \geqslant 0$.

Proof. The coefficients of the SDEs (2.6) are locally Lipschitz in G^0. Then following the Hasminskii theorem on regular solutions of SDEs (see R. Z. Hasminskii (1980)), it is sufficient for proving this proposition to show that there is a twice differentiable with respect to z and once with respect to g Lyapunov function $\mathbf{V}(g, z)$ so that

$$\mathcal{L}\mathbf{V}(g,z) \leqslant c_0 V(g,z) + c_1, \quad (g,z) \in G^0, \tag{B.2}$$

and

$$\lim_{R\to\infty} \inf_{|g|+|z|\geqslant R} \mathbf{V}(g,z) = \infty, \qquad \lim_{g\to 0_+} \mathbf{V}(g,z) = \infty, \tag{B.3}$$

where c_0 and c_1 are constants and $\mathcal{L}$ is the generator for (2.6) given by

$$\mathcal{L} = z\frac{\partial}{\partial g} - \left(\left(D_a + \frac{\bar{B}}{g^3}\right) z + K_z(g - \bar{A})\right)\frac{\partial}{\partial z} + \frac{\sigma^2}{2}\frac{\partial^2}{\partial z^2}. \tag{B.4}$$

It is not difficult to verify that the Lyapunov function

$$\mathbf{V}(g,z) = C_1 z^2 + C_2(\bar{A} - g)^2 + C_3(g - \bar{A})z - \frac{C_4}{g} + \frac{C_5}{g^2}, \tag{B.5}$$

with

$$C_1 > 0, \quad C_2 > 0, \quad C_5 > 0, \quad C_3^2 < 4C_1C_2, \tag{B.6}$$

satisfies the limits in (B.3). Further, choosing

$$C_3 > 0, \quad 2C_1D_a - C_3 \geqslant 0, \quad C_4 = \bar{B}C_3, \quad C_5 = \frac{1}{2}\bar{A}\bar{B}C_3, \quad 2C_1K_z + C_3D_a - 2C_2 = 0, \tag{B.7}$$

we can satisfy (B.2) with $c_0 = 0$ and $c_1 = \sigma^2/2$. □

Remark B.1. *It follows from Proposition 1 that the value of* $g(t)$ *can never reach zero, giving a positive face clearance always, although it may become very small.*

Now, choosing the Lyapunov function $V(g,z) = [z^2/2 + K_z(\bar{A} - g)^2/2]^q$ for any positive integer q, it is not difficult to prove by standard techniques that the moments of the solution to (2.6) are bounded:

$$E\left[\mid g(t) \mid^{2q} + E \mid z(t) \mid^{2q}\right] \leqslant Kt. \tag{B.8}$$

References

Bailey, N.Y., Cliffe, K.A., Hibberd, S. & Power, H. (2013) On the dynamics of a high speed coned fluid lubricated bearing, *IMA Journal of Applied Mathematics,* 79(3): 535-561.

Bailey, N.Y., Cliffe, K.A., Hibberd, S. & Power, H. (2015) Probability of face contact for a high-speed pressurised liquid film bearing including a slip boundary condition, *Lubricants,* 3(3): 493-521.

Bailey, N.Y., Hibberd, S., Tretyakov, M.V. & Power, H. (2017) Dynamics of a small gap gas lubricated bearing with Navier slip boundary conditions, *Journal of Fluid Mechanics,* 818: 68-99.

Bailey, N.Y., Hibberd, S. & Power, H. (2018) Evaluation of the minimum face clearance of a high-speed gas-lubricated bearing with Navier slip boundary conditions under random excitations, *Journal of Engineering Mathematics,* 112(1): 17-35.

Blasiak S. (2015) An analytical approach to heat transfer and thermal distortions in non-contacting face seals, *Int J Heat Mass Transf,* 81: 90-102.

Blasiak S. & and Zahorulko, A.V. (2016) A parametric and dynamic analysis of non-contacting gas face seals with modified surfaces., *Tribology International,* 94: 126-137.

Chen, Y., Peng, X., Jiang, J., Meng, X. and Li, J. (2018) Experimental and theoretical studies of the dynamic behavior of a spiral-groove dry gas seal at high-speeds, *Tribology International,* 125: 17-26.

Crudgington, P., Cross, E. & Cross, R. (2012) A novel high temperature non-contact dynamic seal, *AIAA Paper,* 2012-4004.

Etison, I. (1982) Dynamic analysis of noncontacting face seals, *Transactions of the ASME,* 104:460-468.

Etsion, I. & Burton, R.A. (1979) Observation of self-excited wobble in face seals, *J. Tribology,* 101(4):526-8.

Etsion, I. & Constantinescu, I. (1984) Experimental observation of the dynamic behavior of noncontacting coned-face mechanical seals, *ASLE trans,* 27(3):263-70.

Freidlin, M.I. (1985) Functional integration and partial differential equations, Princeton Univ. Press.

Garratt, J.E., Cliffe, K.A., Hibberd, S. & Power, H. (2012) Centrifugal inertia effects in high speed hydrostatic air thrust bearings, *Journal of Engineering Mathematics,* 76(1): 59-80.

Green, I. (2001) Real-time monitoring and control of mechanical face-seal dynamic behaviour, *Seal Technol,* 2001(96):6-11.

Green, I. (2002) A transient dynamic analysis of mechanical seals including asperity contact and face deformation, *Tribology transactions,* 45(3):284-293.

Green, I. & Etison, I. (1983) Fluid film dynamic coefficients in mechanical face seals, *Journal of Lubrication Technology,* 105:297-302.

Hänggi, P. & Jung, P. (1995) Coloured noise in dynamical systems, *Advances in Chemical Physics,* Vol. LXXXIX, Eds. I. Prigogine and S.A. Rice, Wiley, 239-326.

Hasminskii, R. Z. (1980) Stochastic stability of differential equations, Sijthoff & Noordhoff.

Horsthemke, W. & Lefever, R. (1984) Noise-induced transitions, Springer.

Hou, Z., Zhou, Y., Dimentberg, M.F. & Noori, M. (1996) A stationary model for periodic excitation with uncorrelated random disturbances, *Probabilistic Engineering Mechanics,* 11:191-203.

Huang, H. (2007) Investigation of slip effect on the performance of micro gas bearings and stability of micro rotor-bearing systems, *Sensors,* 7:1399-1414.

Lee, A.S. &, Green, I. (1994) Higher harmonic oscillations in a noncontacting FMR mechanical face seal test rig, *J Vib Acoust,* 116(2):161-7.

Lee, A.S. &, Green, I. (1995) An experimental investigation of the steady-state response of a noncontacting flexibly mounted rotor mechanical face seal, *J Tribol,* 117(1):153-9.

Malanoski, S. & Waldron, W. (1973) Experimental investigation of air bearings for gas turbine engines, *ASLE Transactions,* 16:297-303.

Metcalfe, R. (1982) Dynamic whirl in well-aligned, liquid-lubricated end-face seals withhydrostatic tilt instability, *ASLE trans,* 25(1):1-6.

Milstein, G.N. & Tretyakov, M.V. (2002) The simplest random walks for the Dirichlet problem, *Theory Probab. Appl.,* 47:53-68.

Milstein, G.N. & Tretyakov, M.V. (2004) Stochastic numerics for mathematical physics, Springer.

Park, D.J., Kim, C.H., Jang, G.H. & Lee, Y.B. (2008) Theoretical considerations of static and dynamic characteristics of air foil thrust bearing with tilt and slip flow, *Tribology International,* 41: 282-295.

Salbu, E. (1964) Compressible squeeze films and squeeze bearings, *Transaction of the ASME Journal of Basic Engineering,* 86: 355-366.

San Andrés, L. & Chirathadam, T.A. (2011) Identification of rotordynamic force coefficients of a metal mesh foil bearing using impact load excitations, *Journal of Engineering for Gas and Turbines Power,* 133(11): 112501 1-9.

San Andrés, L. & Kim, T.H. (2008) Analysis of gas foil bearings integrating FE top foil models, *Tribology International,* 42(1),111-120.

Stratonovich, R.L. (1968) Conditional Markov processes and their application to the theory of optimal control, Elsevier.

Varney, P. & Green, I. (2017) Impact phenomena in a noncontacting mechanical face seal, *Journal of Tribology,* 139(2),022201.

Zou, M. &, Green, I. (1999) Clearance control of a mechanical face seal, *Tribol Trans,* 42(3),535-40.

Zou, M., Dayan, J. &, Green, I. (2000) Dynamic simulation and monitoring of a noncontacting flexibly mounted rotor mechanical face seal, *Proc Inst Mech Eng, Part C: J of MechEng Sci,* 214(9),1195-206.

Zou, M., Dayan, J. &, Green, I. (2000) Feasibility of contact elimination of a mechanical face seal through clearance adjustment, *J Eng Gas Turbines Power,* 122(3),478-84.